sigmoidF1: A Smooth F1 Score Surrogate Loss for Multilabel Classification

Anonymous authors
Paper under double-blind review

Abstract

Multilabel classification is the task of attributing multiple labels to examples via predictions. Current models formulate a reduction of the multilabel setting into either multiple binary classifications or multiclass classification, allowing for the use of existing loss functions (sigmoid, cross-entropy, logistic, etc.). These multilabel classification reductions do not accommodate for the prediction of varying numbers of labels per example. Moreover, the loss functions are distant estimates of the performance metrics. We propose *sigmoidF1*, a loss function that is an approximation of the F1 score that (i) is smooth and tractable for stochastic gradient descent, (ii) naturally approximates a multilabel metric, and (iii) estimates both label suitability and label counts. We show that any confusion matrix metric can be formulated with a smooth surrogate. We evaluate the proposed loss function on text and image datasets, and with a variety of metrics, to account for the complexity of multilabel classification evaluation. sigmoidF1 outperforms other loss functions on one text and two image datasets over several metrics. These results show the effectiveness of using inference-time metrics as loss functions for non-trivial classification problems like multilabel classification.

1 Introduction

Many real-world classification problems are challenging because of unclear (or overlapping) class-boundaries, subjectivity issues, and disagreement between annotators. Multilabel learning tasks are common, e.g., document and text classification often deal with multilabel problems (Hull, 1994; Bruno et al., 2013; Yang, 2004; Blosseville et al., 1992), as do query classification (Kang & Kim, 2003; Manning et al., 2008), image classification (Shen et al., 2017; Xiao et al., 2010) and product classification (Amoualian et al., 2020). Existing optimization frameworks typically split the task into known problems and sum over existing losses $\sum \mathcal{L}_{\text{MC}}$, with $\mathcal{L}_{\text{MC}}$ any multiclass classification loss – oftentimes variations of the cross-entropy or logistic loss. Menon et al. (2019) define these as *multilabel reduction* techniques, with an emphasis on two: One-Versus-All (OVA) and Pick-All-Labels (PAL) (Menon et al., 2019). For example, take C as the number of possible classes. OVA and PAL reformulate the multilabel problem to C binary classification and C multiclass classification problems, respectively (see Section 2.3). These methods assume that, for one example, label probabilities (a.k.a. Bayes Optimal Classifier (Dembczyński et al., 2010)) are marginally independent of other label probabilities. Menon et al. show mathematically and empirically that reduction methods (OVA and PAL) can optimize for precision or recall, but not for both precision and recall at once. More generally, a shortcoming shared by OVA and PAL is their reliance on the binary or multiclass classification setting and the lack of a pure multilabel approach. We are not aware of a metric surrogate loss function that deals with multilabel classification in a modern deep learning setting in a single task. Figure 1 illustrates our approach with a concrete example of classifying a movie poster into movie genres with a single loss function: *sigmoidF1*.

Proposed solution to multilabel problems. We propose a loss function $\mathcal{L}_{\widetilde{F1}}$ that (i) naturally approximates the $F1$ classification metric (see Table 3), (ii) estimates label probabilities and label counts (see Eq. 7), and (iii) is decomposable for stochastic gradient descent (see Section 4.1 and Figure 2). Our proposed solution is to use a surrogate of the F1 metric as a loss. Using a metric as a loss function is unpopular for metrics that require a form of thresholding (e.g., counting the number of true positives), as minimizing a step loss function is intractable (Reddi et al., 2019). We resolve this by approximating the step function by a sigmoid curve (see Figure 1).

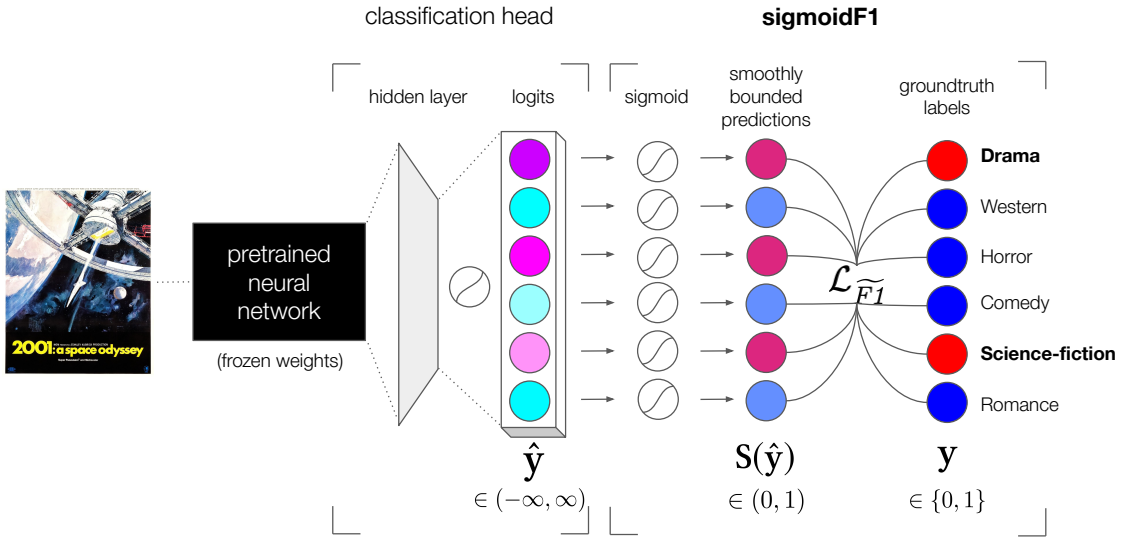

Figure 1: Experimental setup for *sigmoidF1* as a loss function for **multilabel classification**. Here, a movie poster image is fed to a pre-trained network with a custom classification head that outputs logits (i.e., unbounded values) for each class (i.e., movie genre). A sigmoid function forces logits towards either -1 or 1, respectively negative and positive predictions (illustrated by the darker colors). Confusion matrix metrics and F1 can then subsequently be computed. Here, $S(\hat{y}_{horror})$ is close to 1, but the ground truth data claims that *2001: a space odyssey* is not a horror movie; this approximately corresponds to a false positive. Note that $\mathcal{L}_{\widetilde{F1}}$ is computed over a whole batch at training time as a macro measure with the formulas in Sections 4.3 and 4.4. With this setup, one can optimize directly for the metric of interest at training time. Our image and text classification tasks below show improved results when compared to existing losses.

Main contributions. We introduce *sigmoidF1*, an F1 score surrogate, with a sigmoid function acting as a surrogate thresholding step function. *sigmoidF1* allows for the use of the F1 metric that simultaneously optimizes for label prediction and label counts in a single task. *sigmoidF1* is benchmarked against loss functions commonly used in multilabel learning and other existing multilabel models. We show that our custom losses improve predictions over current solutions on several different metrics, across text and image classification tasks. PyTorch and TensorFlow source code are made available.[1]

2 Background

We use a traditional statistical framework as a guideline for multilabel classificaton methods (Tukey, 1977). We distinguish the desired theoretical statistic (the **estimand**), its functional form (the **estimator**) and its approximation (the **estimate**); estimates can be benchmarked with **metrics**. We show how multilabel reduction estimators tend to reformulate the estimand and treat labels as marginally independent. For example, by treating a multilabel problem as a succession of binary classification tasks. However, with a proper estimator, it is possible to directly model the estimand. If F1 score is indeed the statistic of interest (i.e. estimand), our proposed loss function, *sigmoidF1*, accommodates for the true estimand.

We define a learning algorithm $\mathcal{F}$ (i.e., a class of estimators) that maps inputs to outputs given a set of hyperparameters $\mathcal{F}(\cdot;\Theta) : \mathcal{X} \to \mathcal{Y}$. We consider a particular case, with the input vector $\mathbf{x} = \{x_1, \ldots, x_n\}$ and each observation is assigned k labels (one or more) $\mathbf{l} = \{l_1, \ldots, l_C\}$ out of a set of C classes. y_i^j are binary variables, indicating presence of a label for each observation i and class j. Together they form the matrix output $\mathbf{Y}$. This is our multilabel setting. Note that multiclass classification can be considered a subfield of multilabel classification, where a single label is attributed to an example.

[1] `https://anonymous.4open.science/r/sigmoidF1/README.md`

2.1 Estimand and definition of the risk

We distinguish between two scenarios: the *multiclass* and the *multilabel* scenario. In the multiclass scenario, a single example is attributed one class label (e.g., classification of an animal on a picture). In the multilabel scenario, a single example can be assigned more than one class label (e.g., movie genres). We focus on the latter. For a particular set of inputs $\mathbf{x}$ (e.g., movie posters) and outputs $\mathbf{Y}$ (e.g., movie genre(s)), the risk formulation is the same as in (Menon et al., 2019):

$$R_{\mathrm{ML}}(\mathcal{F}) = \mathbb{E}_{(\mathbf{x},\mathbf{Y})}\left[\mathcal{L}_{\mathrm{ML}}(\mathbf{Y}, \mathcal{F}(\mathbf{x}))\right]. \tag{1}$$

The learning algorithm $\mathcal{F}$ is the estimand, the theoretical statistic. For one item x_i, the theoretical risk defines how close the estimand can get to that deterministic output vector $\mathbf{y}_i$. In practice, statistical models do output probabilities $\hat{\mathbf{y}}_i$ via an estimator and its estimate (also called propensities or suitabilities (Menon et al., 2019)). The solution to that stochastic-deterministic incompatibility is either to convert the estimator to a deterministic measure via decision thresholds (e.g., traditional cross-entropy loss), or to treat the estimand as a stochastic measure (our *sigmoidF1* loss proposal).

2.2 Estimator: the functional form

The estimator $f \in \mathcal{F}$ is any minimizer of the risk R_{ML}. Predicting multiple labels per example comes with the assumption that labels are non mutually-exclusive.

Definition. *The multilabel estimator of y_i^j is dependent on the input and other ground truth labels for that example, $\hat{y}_i^j = f(x, y_i^1, \ldots, y_i^{j-1}) = P(y_i^j | y_i^1, \ldots, y_i^{j-1} = 1 | x)$.*

By proposing this general formulation, we entrench that mutually-inclusive characteristic in the estimator. Contrary to Menon et al. (2019), our definition above models interdependence between labels and deals with thresholding for the estimate at training time for free. Waegeman et al. (2014) show that an estimator of an F-score can be used at inference time for multilabel classification, when using probabilistic models where parameter estimation is possible (e.g., decision trees, probabilistic classifier chains). When it is not possible, we resort to defining a loss function.

2.3 Estimate: approximation via a loss function

Most of the literature on multilabel classification can be characterized as multilabel reductions (Menon et al., 2019): an approximation of the original multilabel problem via a loss function $\mathcal{L}(\mathbf{y}_i, f)$. It can take different forms.

One-versus-all (OVA) is a reformulation of the multilabel classification task to a sequence of C binary classifications $(f^1, \ldots, f^C)$, with C the number of classes, $\mathcal{L}_{\mathrm{OVA}}(\mathbf{y}_i, f) = \sum_{c=1}^{C} \mathcal{L}_{\mathrm{BC}}\left(y_i^c, f^c\right)$ where $\mathcal{L}_{\mathrm{BC}}$ is a binary classification loss (binary relevance (Brinker et al., 2006; Tsoumakas & Katakis, 2007; Dembczyński et al., 2010)), most often logistic loss. Minimizing binary cross-entropy is equivalent to maximizing for log-likelihood (Bishop, 2007, §4.3.4).

Pick-all-labels (PAL) gives the loss function $\mathcal{L}_{\mathrm{PAL}}(\mathbf{y}_i, f) = \sum_{c=1}^{C} y_i^c \cdot \mathcal{L}_{\mathrm{MC}}(y_i^c, f)$, with $\mathcal{L}_{\mathrm{MC}}$ a multiclass loss (e.g., softmax cross-entropy). In this formulation, each example $(x_i, \mathbf{y}_i)$ is converted to a multiclass framework, with one observation per positive label. The sum of inherently multiclass losses is used to represent the multilabel estimand.

Multilabel reduction methods are characterized by their way of reformulating the estimand, the resulting estimator, and the estimate. This allows the use of existing losses: logistic loss (for binary classification formulations), sigmoid or softmax cross-entropy loss (for multiclass formulations). These reductions imply a reformulation of the estimator (a.k.a. Bayes Optimal) as follows:

$$\hat{y}_i^j = f(x) = P(y_i^j = 1 | x_i). \tag{2}$$

Contrary to our definition of the original multilabel estimator (Section 2.2), marginal independence of label propensities is assumed. In other words, the loss function becomes any monotone transformation of the

marginal label probabilities $P(y_i^j = 1|x)$ (Dembczyński et al., 2010; Koyejo et al., 2015; Wu & Zhou, 2017). In literature reviews, the multilabel reductions OVA and PAL have been coined as *fit-data-to-algorithm*, as opposed to *fit-algorithm-to-data*. For the purpose of our narrative, we propose the following formalization of this dichotomy: *fit-data-to-algorithm* formulates an additive loss over existing losses $\sum \mathcal{L}_\mathcal{C}$, with $\mathcal{L}_\mathcal{C}$ any classification loss and oftentimes a sum over all classes. This can be contrasted with *fit-algorithm-to-data*, where a custom loss $\mathcal{L}^*$ is built for the multilabel task. We further discuss this in Section 3 and Table 1.

2.4 Metrics: evaluation at inference time

There is consensus on the usefulness of a confusion matrix and ranking metrics to evaluate multilabel classification models at inference time (Koyejo et al., 2015; Behera et al., 2019; Wu & Zhou, 2017). Confusion matrix metrics come with caveats: most of these measures (i) require hard thresholding, which makes them non-differentiable for stochastic gradient descent; (ii) they are very sensitive to the choice of the number top labels to include k (Chen et al., 2006); and (iii) they require aggregation choices to be made in terms of micro/macro/weighted metrics. Common confusion matrix metrics are Precision, Recall, F1-score or one-error-loss; see Wu & Zhou (2017) for others.

2.5 Multilabel estimate: F1 metric as a loss

A model's out-of-sample accuracy is commonly measured on metrics such as AUROC, F1 score, etc. These reflect an objective catered towards evaluating the model over an entire ranking. Due to the lack of differentiability, these metrics cannot be directly used as loss functions at training time (in-sample). Eban et al. (2017) propose a theoretical framework for deriving decomposable surrogates to some of these metrics. We propose our own decomposable surrogates tailored for multilabel classification (see Appendix A).

In a typical machine learning classification task, ground truth binary labels are compared to a probabilistic measure (or a reversible transformation of a probabilistic measure such as a sigmoid or a softmax function) (Bishop, 2007). If the number n_i of labels to be predicted per example is known a priori, it is natural at training time to assign the top_{n_i} predictions to that example (Lapin et al., 2016; 2015). If the number of labels per example is not known a priori, the question remains at both training and at inference time as to how to decide on the number of labels to assign to each example. This is generally done via a *decision threshold*, that can be set globally for all examples (Lipton et al., 2014). This threshold can optimize for specificity or sensitivity (Chen et al., 2006) – for per-class thresholding see Chu & Guo (2017). In Section 4, we propose an approach where this threshold is implicitly defined at training time, by using a loss function that penalizes explicitly for wrong label counts and fits to the original estimand in Definition 2.2: the F1 metric. In Section 4, we show how F_1 is formulated into a surrogate loss $\mathcal{L}_{\widetilde{F1}}$. Our contribution is thus in the continuation of the *fit-algorithm-to-data* trend, because we propose a custom loss function. That loss function is also the first to directly approximate the F1 score with non-divergent estimates (see Sections 4.1 and 4.2 on *boundedness*).

3 Related Work

In Section 2.3, we mentioned how existing solutions for multilabel tasks can be divided into *fit-data-to-algorithm* solutions, which map multilabel problems to a known problem formulation like multiclass classification, and *fit-algorithm-to-data* solutions, which adapt existing classification algorithms to the problem at hand (Madjarov et al., 2012). In most of this work, the term *multilabel classification* excludes *extreme* (tens of thousands of labels) (e.g., Jernite et al., 2017; Agrawal et al., 2013; Jain et al., 2019), *hierarchical* (parent and children labels) (e.g., Lehmann et al., 2015; Yang et al., 2019; Howard & Ruder, 2018) or *multiclass* (single label per example) subfields. These subfields call for their own solutions, including label embeddings (Bhatia et al., 2015) or negative mining (Reddi et al., 2019) for the *extreme* usecase.

Fit-data-to-algorithm. In fit-data-to-algorithm solutions, cross-entropy losses (Fisher, 1912; Good, 1952) are used at training time and thresholding is done at inference time to determine how many labels should be assigned to an instance. This has also been called multilabel reduction (Menon et al., 2019) and differs from multiclass-to-binary classifications (Zhang, 2004; Tewari & Bartlett, 2005; Ramaswamy et al., 2014). We can

Table 1: *SigmoidF1* and related loss formulations. The solution column refers to our proposed formalization of the literature review on how to conduct multilabel classification: *D2A* refers to *fit-data-to-algorithm* (sum over existing or cross-entropy-like, CE-like, classification losses $\sum \mathcal{L}_{\mathcal{C}}$) and *A2D* refers to *fit-algorithm-to-data* (custom loss $\mathcal{L}^*$)

Method	Solution	Model type	Context	Implementation	Surrogated metric	Modality
BCE [1912]	*D2A*	Any	Any	CE-like	–	Any
MFC [2015]	–	Gaussian mixtures	Mispronunciation detection	sigmoid	F_1	Text
optLosses [2017]	*A2D*	Any	Any	–	F_1	Theoretical
focalLoss [2017]	*D2A*	Neural net	Imbalanced-multiclass	CE-like	–	Image
softF1 [2019]	*A2D*	Neural net	Multilabel	Unbounded	F_1	Image
ASL [2020]	*D2A*	Neural net	Multilabel	CE-like	–	Image
RS@k [2022]	*A2D*	Neural net	Similarity	sigmoid	Recall	Image
polyLoss [2022]	*A2D*	Neural net	Imbalanced-multiclass, ...	CE-like	–	Image
sigmoidF1 [ours]	*A2D*	Neural net	Multilabel	sigmoid	F_1	Text & Image

further distinguish between One-versus-all (OVA) and Pick-all-labels (PAL) solutions (Menon et al., 2019) (see Section 2). In OVA, one reduces the classification problem to independent binary classifications (Brinker et al., 2006; Tsoumakas & Katakis, 2007; Dembczyński et al., 2010; Wydmuch et al., 2018). In PAL, one reformulates the task to independent multiclass classifications (Boutell et al., 2004; Jernite et al., 2017; Joulin et al., 2017). The *label powerset* approach considers each set of labels as a class (Boutell et al., 2004). In Pick-One-Label (POL), a single multiclass example is created by randomly sampling a positive label (Joulin et al., 2017; Jernite et al., 2017). Alternatively, *ranking by pairwise comparison* is a solution where the dataset is duplicated for each possible label pair. Each duplicated dataset has therefore two classes and only contains instances that have at least one of the labels in the label pair. Different ranking methods exist (Hüllermeier et al., 2008; Loza Mencia & Furnkranz, 2008). More recently, hierarchical datasets such as DBpedia (Lehmann et al., 2015) are used to fine-tune BERT-based models (Yang et al., 2019; Zaheer et al., 2020); the latter publications use cross-entropy to predict the labels.

Fit-algorithm-to-data. In fit-algorithm-to-data solutions, elements of the learning algorithm are changed (e.g., the back propagation procedure). Early representatives stem from heterogenous domains of machine learning. MultiLabel k-Nearest Neighbors (Zhang & Zhou, 2007), MultiLabel Decision Tree (Clare & King, 2001), Ranking Support Vector Machine (Elisseeff & Weston, 2001) and Backpropagation for MultiLabel Learning (Zhang & Zhou, 2006). More recently, the idea of multi-task learning for *label prediction* and *label count prediction* was introduced (ML_{NET}, Du et al., 2019; Li et al., 2017; Wu et al., 2019). The literature has been clearly hinting at the usefulness of a single task loss function that approximates a metric. A formulation similar to our loss *unboundedF1* was proposed in an unpublished blog post, which was referred to as *softF1* (Chang et al., 2019). Outside of the context of neural networks, the *Maximum F1-score criterion* for automatic mispronunciation detection was proposed as an objective function to a Gaussian Mixture Model-hidden Markov model (GMM-HMM) (Huang et al., 2015). A recent paper used recall as a loss function for image similarity (Patel et al., 2022). In parallel, there is a growing consensus that the original cross-entropy loss (*fit-data-to-algorithm*) cannot solve all our problems. A variation of the cross-entropy loss adapted to multilabel classification has been proposed (Baruch et al., 2020; Wu et al., 2019); it extends the multiclass sparse class representation setting (Lin et al., 2017; Leng et al., 2022). In the ranking domain, LambdaLoss has been proposed to optimize directly for the lambdaRank metric (Wang et al., 2018). In the theoretical space, Eban et al. (2017) have proposed a generic framework for decomposable metrics, including $F1$ as a theoretical fractional linear program. Table 1 illustrates how *sigmoidF1* differs from the methods listed in this paragraph.

An important limitation shared by existing *fit-data-to-algorithm* and *fit-algorithm-to-data* approaches is the lack of a unified loss framework that deals with multilabel classification and can approximate a metric of interest. *sigmoidF1* computes an F1 surrogate loss over the aggregation of examples in a batch at training time.

4 Method

We introduce our approach for multilabel problems, with a smoothed confusion matrix metric as a loss (the original confusion matrix metrics rely on step functions and are therefore intractable, see for example the blue step function in Figure 2). We first briefly define our learning setting and define the confusion matrix metrics in this setting more formally.

We use the binary classification setting (two classes) to simplify notation, without loss of generalization to the multilabel case. In a typical binary classification problem with the label vector $\mathbf{y} = \{y_1, \ldots, y_n\}$, predictions are probabilistic and it is necessary to define a threshold t, at which a prediction is binarized. With $\mathbb{1}$ as an indicator function, $\mathbf{y}^+ = \sum \mathbb{1}_{\hat{\mathbf{y}} \geq t}$, $\mathbf{y}^- = \sum \mathbb{1}_{\hat{\mathbf{y}} < t}$ are thus the count of positive and negative predictions at threshold t. Let *tp*, *fp*, *fn*, *tn* be number of true positives, false positives, false negatives and true negatives respectively:

$$\begin{aligned} tp &= \sum \mathbb{1}_{\hat{\mathbf{y}} \geq t} \odot \mathbf{y} \quad fp = \sum \mathbb{1}_{\hat{\mathbf{y}} \geq t} \odot (\mathbb{1} - \mathbf{y}) \\ fn &= \sum \mathbb{1}_{\hat{\mathbf{y}} < t} \odot \mathbf{y} \quad tn = \sum \mathbb{1}_{\hat{\mathbf{y}} < t} \odot (\mathbb{1} - \mathbf{y}), \end{aligned} \tag{3}$$

with $\odot$ the component-wise multiplication sign. For simplicity, in the formulation above and the ones that follow scores are calculated for a single class, therefore the sum is implicitly over all examples $\sum_i$. This applies to the binary classification problem but also to our multilabel setting, when micro metrics are calculated (i.e., compute the metric value for each class, and then averaged over all classes). In the multilabel setting $\mathbf{y}$ can be substituted by $\mathbf{y}^j$ for each class j. Note that vectors could be trivially substituted by matrices ($\mathbf{Y}$) in Eq. 3 to obtain the macro formulation. Given the four confusion matrix quadrants, we can generate further metrics like precision and recall (see Table 4 in Appendix A). However, none of these metrics are decomposable due to the hard thresholding, which is, in effect, a step function (see Figure 2).

Next, we define desirable properties for decomposable thresholding, unbounded confusion matrix entries and a sigmoid transformation that renders confusion matrix entries decomposable. Finally, we focus on a smooth F1 score.

4.1 Desirable properties of decomposable thresholding

We define desirable properties for a decomposable sign function $f(u)$ as a surrogate of the above indicator function $\mathbb{1}_{\hat{\mathbf{y}} < t}$.

Property 1. *Boundedness: $|f(u)| < M$, where M is an upper and lower bound.*

The ground truth $\mathbf{y}$ is bounded between $[0, 1]$ and thus it must be compared to a bounded prediction $\hat{\mathbf{y}}$, preferably bounded by $[0, 1]$, to avoid further scaling.

Property 2. *Saturation: $\int_s^\infty f^{-1}(u) = \int_{-\infty}^{-s} f(u) = \epsilon$, with ϵ a number close to zero and s a saturation bound.*

For the surrogate to be a proper sign function substitute, it is important to often return values close to 1 or 0. Saturation is defined in the context of neural network activation functions and refers to the propensity of iterative backpropagation to progressively lead to values very close to 0 or 1 after a long enough training period. Our aim is to reach that convergence quickly in order to force decisions towards 0 or 1 in order to be comparable to a step function. This highlights a tension: the sigmoid function should contrast outputs towards 0 or 1 but should not be too saturated, in order for the derivative at point u to be non-null and information to flow back to the network (Krizhevsky et al., 2017).

Property 3. *Dynamic Gradient: $f'(u) \gg 0 \quad \forall\, u \in [-s, s]$, where s is the saturation bound.*

Inside the saturation bounds $[-s, s]$, the derivative should be significantly higher than zero in order to facilitate stochastic gradient descent and backpropagation. Note that the upper and lower limits of $f(u)$ are interchangeably $[-1, 1]$ or $[0, 1]$ along this paper and in literature. The conditions above still apply by linear transformation. Next, we show how our formalization of an unbounded F1 surrogate would not fulfill these properties and how our proposition of a smooth bounded alternative does.

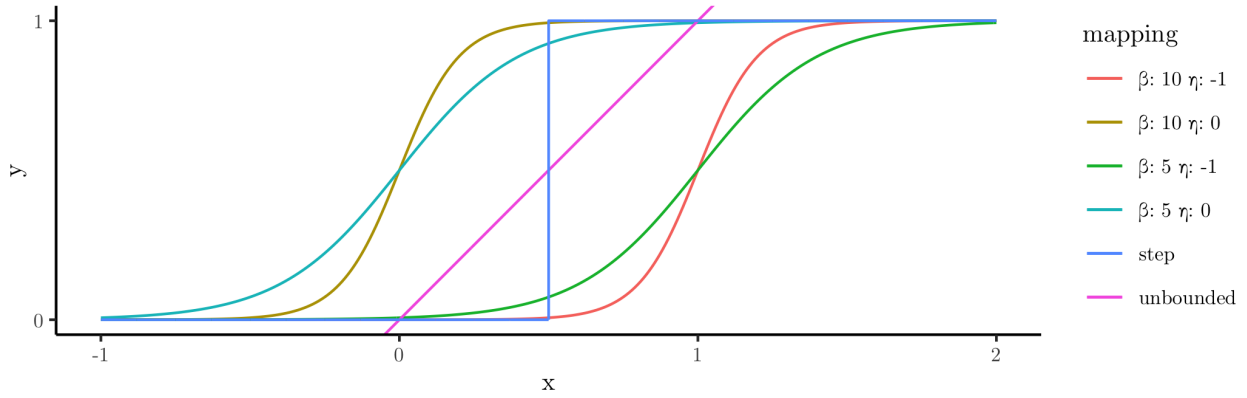

Figure 2: Different thresholding regimes: the step function (original *F1* metric) is not decomposable, the linear function is unbounded ($\mathcal{L}_{\overline{F1}}$) and tends to produce divergent gradients, whereas the sigmoid function ($\mathcal{L}_{\widetilde{F1}}$) is bounded and allows for differentiation due to its smooth curvature, tunable at different parametrizations.

4.2 Unbounded confusion matrix entries

A first trivial remedy to allow for derivation of the sign function $f(u)$, is to define *unbounded* confusion matrix entries by retaining the original logits (scores) when counting true positives, false negatives, etc. Countrary to the original confusion matrix definition in Eq. 3, $\overline{tp}$, $\overline{fp}$, $\overline{fn}$ and $\overline{tn}$ are not natural numbers anymore:

$$\begin{aligned} \overline{tp} &= \sum \hat{\mathbf{y}} \odot \mathbf{y} & \overline{fp} &= \sum \hat{\mathbf{y}} \odot (\mathbb{1} - \mathbf{y}) \\ \overline{fn} &= \sum (\mathbb{1} - \hat{\mathbf{y}}) \odot \mathbf{y} & \overline{tn} &= \sum (\mathbb{1} - \hat{\mathbf{y}}) \odot (\mathbb{1} - \mathbf{y}), \end{aligned} \tag{4}$$

where *tp*, *fp*, *fn* and *tn* are now replaced by rough surrogates. The disadvantages are that the desirable properties mentioned above are not fulfilled, namely (i) $\hat{\mathbf{y}}$ is unbounded and thus certain examples can have over-proportional effects on the loss; (ii) it is non-saturated; while non-saturation is desirable for activation functions (Krizhevsky et al., 2017), here it would be desirable to tend towards saturation (i.e., tend to values close to 0 or 1, so as to give the most accurate predictions at any thresholding values at inference time); and (iii) the gradient of that linear function is 1 and therefore backpropagation will not learn depending on different inputs at this stage of the loss function. However, this method has the advantage of resulting in a linear loss function that avoids the concept of thresholding altogether and is trivial to decompose for stochastic gradient descent.

4.3 Smooth confusion matrix entries

We propose a sigmoid-based transformation of the confusion matrix that renders its entries decomposable and fulfills the three desirable properties above:

$$\begin{aligned} \widetilde{tp} &= \sum \mathbf{S}(\hat{\mathbf{y}}) \odot \mathbf{y} & \widetilde{fp} &= \sum \mathbf{S}(\hat{\mathbf{y}}) \odot (\mathbb{1} - \mathbf{y}) \\ \widetilde{fn} &= \sum (\mathbb{1} - \mathbf{S}(\hat{\mathbf{y}})) \odot \mathbf{y} & \widetilde{tn} &= \sum (\mathbb{1} - \mathbf{S}(\hat{\mathbf{y}})) \odot (\mathbb{1} - \mathbf{y}), \end{aligned} \tag{5}$$

with $\mathbf{S}(\cdot)$ the vectorial form of the sigmoid function $S(\cdot)$:

$$S(u; \beta, \eta) = \frac{1}{1 + \exp(-\beta(u + \eta))}, \tag{6}$$

with β and η tunable parameters for slope and offset, respectively. Higher β results in steeper slope at the center of the sigmoid and thus more stringent thresholding. At its extreme, $\lim_{\beta \to \infty} S(u; \beta, \eta)$ corresponds to the step function used in Eq. 3. Note that negative values of β geometrically reflect the sigmoid function across the horizontal line at 0.5 and thus invert predictions. These smooth confusion matrix entries allow us

to build any related metric (see Table 4 in Appendix A). Furthermore, the surrogate entries are decomposable, bounded, saturated and have a dynamic gradient.

4.4 Smooth macro F1 scores

F1 scores can be calculated on a macro and micro level. Macro-averaging regards all classes as equally important, whereas micro-averaging reflects within-class frequency. *unboundedF1* and *sigmoidF1* below are thought of as macro scores (aggregated over all classes). These scores require a high enough number of representatives in the four confusion matrix quadrants to learn from batch to batch. Ideally, each training epoch would have only one batch, so as to have the most representatives. Following Eq. 4, it is possible to define an *unbounded F1* score:

$$\mathcal{L}_{\overline{F1}} = \frac{2\overline{tp}}{2\overline{tp} + \overline{fn} + \overline{fp}}. \tag{7}$$

While this alternative abstracts the thresholding away, which is convenient for fine-tuning purposes, it does not fulfill the desirable properties of a binarization threshold surrogate (see Section 4.2). *unboundedF1* will be used to benchmark against our proposed *sigmoidF1* loss. Given the definitions of smooth confusion matrix metrics above, we can now write $\mathcal{L}_{\widetilde{F1}}$:

$$\mathcal{L}_{\widetilde{F1}} = \frac{2\widetilde{tp}}{2\widetilde{tp} + \widetilde{fn} + \widetilde{fp}}. \tag{8}$$

sigmoidF1 is particularly suited for the multilabel setting because it is a proper hard thresholding surrogate as defined in the previous sections and because it contains a significant amount of information about label prediction accuracy: $\widetilde{tp}$, $\widetilde{fn}$ and $\widetilde{fp}$ are indicative of the number of predicted labels in each category of the confusion matrix but also contain a notion of certainty, given that they are rational numbers. The built in sigmoid function ensures that certainty increases along training epochs, as outlined by Property 2. Finally, as the harmonic mean of precision and recall (a property of F1 in general), it weighs in both relevance metrics.

In the next section, we implement Eq. 8 in PyTorch and TensorFlow as a custom loss as follows:

```
# with y the ground truth and z the outcome of the last layer
sig = 1 / (1 + exp(β * (z + η)))
tp = sum(sig * y, dim=0)
fp = sum(sig * (1 - y), dim=0)
fn = sum((1 - sig) * y, dim=0)
sigmoid_f1 = 2*tp / (2*tp + fn + fp + 1e-16)
```

The pseudocode above illustrates the elementwise multiplication of matrices $\mathbf{S}(\hat{\mathbf{y}})$ and $\hat{\mathbf{y}}$ over all examples in the batch and all possible classes.

5 Experimental Setup

We test multilabel learning using our proposed *sigmoidF1* loss function on three datasets across different modalities (image and text). For each modality we take a state-of-the-art model that generates an embedding layer and append a sigmoid activation and different losses. Multilabel deep learning is usually implemented with sigmoid binary cross-entropy directly on the last neural layer (a simplification of the OVA and PAL reductions). We follow this approach for our experiments (e.g., in (large) language models (Zaheer et al., 2020; Devlin et al., 2019)). Some baselines include multilabel reformulation choices: only keeping the top-n occurring classes (often 4–10) (e.g., Zhang et al., 2015; Cunha et al., 2021), multiclass classification on each entity within an example (objects in an image, expressions in a text) (e.g., Lin et al., 2014; Wang et al., 2016; Wei et al., 2016; Zhu et al., 2017). We refrain from doing so.

5.1 Datasets

Two of the datasets that we use are multilabel in nature. moviePosters is related to movies (Neha, 2018) and arXiv2020 relates to arXiv paper abstracts (Cornell-University, 2021). In addition, we use the image

Table 2: Descriptive statistics of our experimental datasets.

	Type	Classes	Average label count	Number of examples
moviePosters	image	28	2.165	37,632
arXiv2020	text	155	1.888	26,558
Pascal-VOC	image	20	1.560	9,963

segmentation dataset Pascal-VOC (Everingham et al., 2007), with bounding boxes and one label per box. By attributing all box labels to the image as a whole, it has been used as a reference benchmark for multilabel classification. We refer to Appendix C for further descriptions of the datasets and references.

5.2 Learning framework

Our proposed learning framework consists of two parts: a pretrained deep neural network and a classification head (see Figure 1); different loss functions are computed in the classification head.

Neural network architecture For the moviePoster image dataset, we use a MobileNetV2 (Sandler et al., 2018) architecture that was pretrained on ImageNet (Deng et al., 2009). This network architecture is typically used for inference on small computing devices (e.g., smartphones). We use a version of MobileNetV2 already stripped off of its original classification head (Google, 2021). For the three text datasets, we use DistilBERT (Sanh et al., 2019) as implemented in Hugging Face. This is a particularly efficient instance of the BERT model (Huggingface, 2021). For the Pascal-VOC dataset, we use the recent state-of-the-art resnet TresNet (Ridnik et al., 2021) pretrained on ImageNet (Deng et al., 2009) and some of the best practices for Pascal-VOC collected in a recent benchmark (Baruch et al., 2020). We use TresNet-m-21K; 21K stands for Imagenet21K, the larger ImageNet corpus. In all cases, we use the final pre-trained layer as an embedding of the input. To ensure that the results of different loss functions are comparable, we fix the model weights of the pretrained MobileNetV2, DistilBERT and TresNet and keep the hyperparameter values that were used to be trained from scratch. At training time, we optimize with Adam for all three architectures and use In-Place Activated BatchNorm (Inplace-ABN) for TresNet Rota Bulò et al. (2018).

The **classification head** is a latent representation layer (the final pretrained layer mentioned above) connected with a RELU activation. This layer is linked to a final classification layer with a linear activation. The dimension of the final layer is equal to the number of classes in the dataset. The attached loss function is either BCE (Binary Cross-Entropy), focalLoss (Lin et al., 2017), ASL (Baruch et al., 2020), unboundedF1 or sigmoidF1 (ours). When computing the loss at training time, a sigmoid transforms the unbounded last layer to a $[-1, 1]$ bounded vector that contrasts positive and negative predictions. These values are then used as inputs to any of the loss functions above over all classes and the entire batch of examples. In the case of $\mathcal{L}_{\widetilde{F1}}$, this corresponds to a surrogate macro F1. Given the vectorized computation of $\mathcal{L}_{\widetilde{F1}}$ (see Section 4.3), the computational burden is only marginally affected. At inference time, the last layer is used for prediction and is bounded with a sigmoid function. A threshold must then be chosen at evaluation time to compute different metrics. Figure 1 depicts this learning framework.

Metrics In our experiments, we report on microF1, macroF1, Precision, mAP (used in some recent multilabel benchmarks; see Appendix A) and (micro-)weightedF1 (where within-class scores are weighted by their representation in the dataset). We focus our discussion around weightedF1 as it is the most comprehensive F1 measure we could find on multilabel problems. Given limited resources we rerun each model on each loss with 5 random seeds. With only 5 runs per loss function, hypothesis testing results would have been particularly sensitive to the choice of distribution.[2] Instead we show the distribution of results in Appendix D, which show robust statistics (median and interquartile range). Note that cross-validation cannot be performed as Pascal-VOC has fixed train-validation-test sets. There is an interaction between our optimization on *sigmoidF1* and our evaluation using (weighted) F1 metrics. We expect higher values on F1-related metrics during evaluation and thus report on alternative metrics too.

[2]We found that, given some unstable results on unboundedF1, even a conservative student t distribution would imply that the 95% confidence interval covers metric values over 100%

5.3 Hyperparameters and reproducibility

We implemented all losses in Pytorch and Tensorflow. Batch size is set at a relatively high value of 256 to increase accuracy over traditional losses (Smith et al., 2017), but also allow heterogeneity in the examples within the batch, thus collecting enough values in each quadrant of the confusion matrix (see Section 4.4 for a discussion). Regarding the *sigmoidF1* hyperparameters β and η, we performed a grid search with the values in the range $[1, 30]$ for β and $[0, 2]$ for η. In our experiments, we evaluate the sensitivity of our method to these hyperparameters (see Figure 2 and Appendix C for optimal values). We made sure to split the data in the same training, validation and test sets for each loss function. We trained for 60 (Pascal-VOC) to a 100 (arXiv2020, moviePosters) epochs, depending on convergence. Our code, dataset splits and other settings are shared to ensure reproducibility of our results.

6 Experimental Results

The goal of *sigmoidF1* ($\mathcal{L}_{\widetilde{F1}}$) is to optimize for the F1 score directly at training time in the context of multilabel classification. In this section, we test whether $\mathcal{L}_{\widetilde{F1}}$ can outperform existing loss functions on multiple classification metrics. We present multilabel classification results for $\mathcal{L}_{\widetilde{F1}}$ on three datasets, moviePosters, arXiv2020 and Pascal-VOC in Table 3.

We recall Table 1, in which we highlight that $\mathcal{L}_{\text{BCE}}$ is originally designed for binary classification, $\mathcal{L}_{\text{FL}}$ for imbalanced multiclass, $\mathcal{L}_{\text{ASL}}$ to optimize mAP for multilabel classification. They are computed over each class at training time, as opposed to per batch for our $\mathcal{L}_{\widetilde{F1}}$ and $\mathcal{L}_{\overline{F1}}$. The latter two explicitly account for label dependencies in the loss function.

In general, Table 3 shows that $\mathcal{L}_{\widetilde{F1}}$ outperforms other loss functions on three possible formulations of the F1 metric (weightedF1, microF1 and macroF1). We also confirm that the recent ASL loss outperforms other losses on the precision and mAP metrics. $\mathcal{L}_{\widetilde{F1}}$ is designed as an F1 surrogate, it is thus not surprising for it to perform best on F1 metrics and comes at no noticeable additional computational cost (see Appendix E). We first analyze the F1 metrics before interpreting the precision and mAP results in more detail.

Measured on the F1 metrics (weightedF1, microF1 and macroF1), $\mathcal{L}_{\widetilde{F1}}$ and $\mathcal{L}_{\text{BCE}}$ always share the top 2 in performance, oftentimes far ahead of other losses. This highlights that losses inspired by BCE are not yet tailored to optimize for the F1 score in multilabel classification, and also that BCE is a good default choice in general. However, in certain settings, and in particular with our bigger dataset Pascal-VOC, $\mathcal{L}_{\widetilde{F1}}$ can provide clear improvements over the original BCE. macroF1 on the moviePosters dataset is a counter-intuitive exception to that observation: BCE outperforms $\mathcal{L}_{\widetilde{F1}}$ only on the macro measure, although $\mathcal{L}_{\widetilde{F1}}$ is essentially a macro F1 loss function, as it is calculated across all classes and over each entire batch.

On precision and mAP, no top 2 losses emerge. Instead, results are dataset and modality dependent. Surprisingly, the traditional BCE loss outperforms other losses by far in precision on a thoroughly benchmarked dataset like Pascal-VOC. Precision performance gains are less clear on the two smaller datasets (arXiv2020 and moviePosters); $\mathcal{L}_{\overline{F1}}$ performs reasonably well.[3] Regarding mAP, $\mathcal{L}_{\text{ASL}}$ expectedly outperforms other methods on Pascal-VOC, confirming their own benchmarks (Baruch et al., 2020). Notably, $\mathcal{L}_{\text{ASL}}$ is also first on mAP on text data. This is the first time that ASL is tested on text data to the best of our knowledge. Overall, these mitigated results for precision and mAP motivate further research in optimizing directly for precision and mAP at training time.

A note on thresholding and zero values. For the bigger and more standard dataset Pascal-VOC,[4] our neutral metric threshold of 0.5 provides results in line with the literature. With our own fine-tuning regime on a smaller model (see Section 5.2), our mAP scores are 1–2% away from the current state of the art (Baruch et al., 2020). On smaller datasets like arXiv2020, moviePosters and others (see Appendix F), the sigmoid activation per class at inference time are closer to zero. To a certain extent, this can be interpreted

[3] $\mathcal{L}_{\overline{F1}}$ was found particularly unstable for Pascal-VOC over 5 different seeds (see the extended results in Appendix D). Provided it is unbounded, predictions can diverge towards (positive or negative) infinite values.

[4] The classes in Pascal-VOC are a lot more concrete (e.g., car, person, bicycle) and are directly related to the original classes of ImageNet on which the TresNet and MobileNetV2 were trained, as opposed to movie genres for moviePosters or arXiv paper scientific domain.

Table 3: Multilabel classification mean performance in percent over 5 random seeds. The F1 metric variants are the focus here (weightedF1, microF1 and macroF1), since we aim to directly optimize for F1 at training time. precision and mAP are displayed for reference, as they are often used in the literature in that context. Metric are formally defined in Appendix A and thresholds are indicated there for each dataset.

	Loss	**weightedF1**	**microF1**	**macroF1**	precision	mAP
TresNetm21K [2021] on Pascal-VOC @0.5 (CNN)	$\mathcal{L}_{\text{BCE}}$[1912]	87.52	85.85	87.76	**90.75**	91.54
	$\mathcal{L}_{\text{FL}}$[2017]	72.54	59.24	76.82	84.70	76.19
	$\mathcal{L}_{\text{ASL}}$[2020]	77.85	76.53	75.98	65.36	**93.11**
	$\mathcal{L}_{\overline{FI}}$[ours]	77.24	74.84	75.31	75.53	79.36
	$\mathcal{L}_{\widetilde{FI}}$[ours]	**88.20**	**87.70**	**87.87**	85.36	92.36
DistilBert [2019] on arXiv2020 @0.05 (NLP)	$\mathcal{L}_{\text{BCE}}$[1912]	20.59	18.19	18.42	10.15	10.50
	$\mathcal{L}_{\text{FL}}$[2017]	18.85	16.59	18.01	10.10	10.43
	$\mathcal{L}_{\text{ASL}}$ [2020]	19.15	16.90	18.16	**10.32**	**10.53**
	$\mathcal{L}_{\overline{FI}}$[ours]	15.23	13.74	14.50	10.27	10.49
	$\mathcal{L}_{\widetilde{FI}}$[ours]	**20.60**	**18.20**	**18.43**	10.15	10.50
MobileNetV2 [2018] on moviePosters @0.05 (CNN)	$\mathcal{L}_{\text{BCE}}$[1912]	13.79	9.47	**12.94**	5.51	5.78
	$\mathcal{L}_{\text{FL}}$[2017]	0.00	0.00	0.00	0.00	5.80
	$\mathcal{L}_{\text{ASL}}$[2020]	0.00	0.00	0.00	0.00	5.80
	$\mathcal{L}_{\overline{FI}}$[ours]	13.97	9.84	10.11	**5.59**	**5.90**
	$\mathcal{L}_{\widetilde{FI}}$[ours]	**14.81**	**10.33**	10.57	5.58	5.81

as the model having less confidence in its predictions (Guo et al., 2017). As a result, a neutral 0.5 threshold resulted in zero values on almost all losses and metrics for small datasets. Given the range of values in these predictions, 0.05 seems like the next best neutral threshold. We refrain from further finetuning the threshold for each dataset, loss and metric.[5] As a result of the absence of finetuning, moviePosters display zero values for $\mathcal{L}_{\text{FL}}$ and $\mathcal{L}_{\text{ASL}}$ on most metrics. This can be explained by the higher average label count for moviePosters. This is in opposition to the propensity of $\mathcal{L}_{\text{FL}}$ and $\mathcal{L}_{\text{ASL}}$ to deal with sparser label representation.

The analysis above highlights that sigmoidF1 can indeed optimize for F1 metrics (weightedF1, microF1 and macroF1) reliably and consistently, over five datasets in total (see Appendix D). Given the more mitigated results for precision and mAP, it seems relevant to further explore opportunities of metrics-as-losses. Finally, BCE, which was designed with binary classification in mind, is a good first approximation.

Sensitivity analysis. In Figure 3, we show the sensitivity of *sigmoidF1* to different parametrizations of η and β. Within the chosen values (see Section 5.3), we chose to display a parameter space similar to the one illustrated in Figure 2. Moving the sigmoid to the left allows the learning algorithm to tend to a (local) optimum. In general and across datasets, when sampling for η, we noticed how the optimum tended towards positive values. Offsetting the sigmoid curve to the left has the effect of pushing more candidate predictions to the rank of positive instance (or at least close to 1). We also note how β (which cannot be negative or otherwise the sigmoid function would flip around the horizontal axis) is at best close to a value close to 0 on this dataset (we show discrete values here for display purposes). The sigmoid is thus relatively smooth, which involves dynamic gradients over different batches. The idea is similar to a high learning rate. In our experiments, this rarely gave rise to divergent behavior in the loss function (learning curve). We learn that it is necessary to tune hyperparameters for each dataset, as it is for $\mathcal{L}_{\text{FL}}$, $\mathcal{L}_{\text{ASL}}$ and others in Table 1.

The results in this section show that, in general, multilabel classification results measured on F1 metrics can be improved using sigmoidF1 – independently of the dataset, its modality or the neural network architecture.

[5]While optimizing the threshold at inference time is an interesting research topic, we refrain from doing so here, so as to disantangle the loss function benchmarking from the thresholding regime benchmarking.

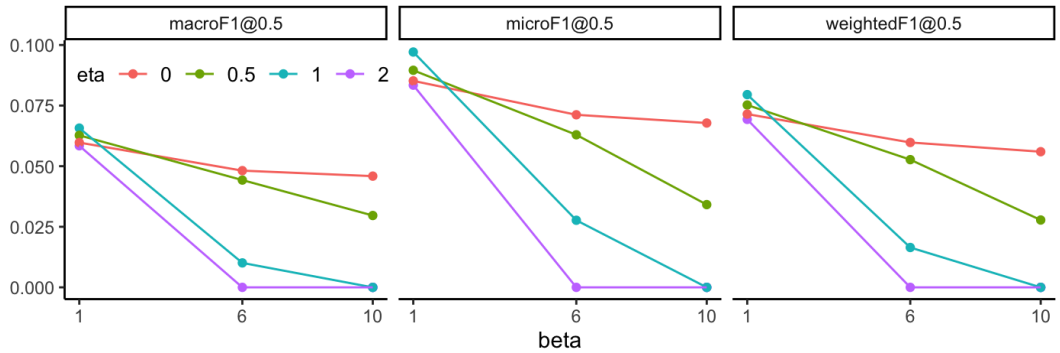

Figure 3: DistilBERT (NLP) on arXiv2020 – different weightedF1 scores at a 0.5 threshold for different values of η and β in a sampling region similar to Figure 2.

7 Conclusions

To solve multilabel learning tasks, existing optimization frameworks are typically based on variations of the cross-entropy loss. Instead, we propose the *sigmoidF1* loss, as part of a general loss framework for confusion matrix metrics. *sigmoidF1* loss can achieve significantly better results for most metrics on three diverse datasets and outperforms other losses on the weightedF1 metric. We thereby provide evidence that *sigmoidF1* is robust to modality, model architecture and dataset size, when optimizing for F1 metrics. Generally, our smooth formulation of confusion matrix metrics allows us to optimize directly for these metrics that are usually reserved for the evaluation phase. The proposed *unboundedF1* counterpart does not require hyperparameter tuning and delivered better results than existing multiclass losses on most metrics; it can act as a mathematically less robust approximation of *sigmoidF1*.

In future work and within the generic multilabel setting, a first incremental step could be to train on a bigger dataset like MS-COCO (Lin et al., 2014) (if provided with more resources) and use more robust transfer learning/finetuning procedures, for example with dynamic weight freezing for finetuning (Howard & Ruder, 2018). Alternatively, we could train a CNN or a BERT model for multilabel tasks with our smooth losses from scratch (cf., (Wu et al., 2019) and (Lin et al., 2017)). If training from scratch, this can be combined with representation learning (Milbich et al., 2020; Wang et al., 2020) or self-supervised learning, in order to model abstract relationships.

Next, we could validate if F1 or another confusion-matrix-metric-as-a-loss can tackle other multilabel settings, such as hierarchical multilabel classification (Benites & Sapozhnikova, 2015), active learning (Nakano et al., 2020), multi-instance learning (e.g., Soleimani & Miller, 2017; Zhou et al., 2012), holistic label learning (see dataset *Large Scale Holistic Video Understanding* (Diba et al., 2019)), or extreme multilabel prediction (Chang et al., 2020; Liu et al., 2017; Babbar & Schölkopf, 2017; Yen et al., 2017; Prabhu et al., 2018) (with missing labels (Yu et al., 2014; Jain et al., 2016)), where the number of classes ranges in the tens of thousands. Beyond the multilabel setting, *sigmoidF1* could be tested on any model that uses F1 score as an evaluation metric such as AC-SUM-GAN (Apostolidis et al., 2020).

One limitation of *sigmoidF1* is that it is computed at a macro level over the whole batch and ignores (micro) per class F1 scores. Given our limited GPU memory, we could not load enough examples in each batch to represent each confusion matrix quadrant of each class reliably. If such a route is followed, we could eventually finetune or learn β_c and η_c – the parameters of the sigmoid function – per class c.

We believe that smooth metric surrogates should inform future research on multilabel classification tasks. There is evidence of a growing interest in the literature (Chang et al., 2019; Huang et al., 2015; Patel et al., 2022) for metrics as losses and the objective of this paper is to further highlight their relevance, across modalities, architectures and dataset sizes. Based on the results presented in this paper, we consider metrics-as-losses as the next step in the evolution of multilabel classification algorithms.

References

Martín Abadi, Ashish Agarwal, Paul Barham, Eugene Brevdo, Zhifeng Chen, Craig Citro, Greg S. Corrado, Andy Davis, Jeffrey Dean, Matthieu Devin, Sanjay Ghemawat, Ian Goodfellow, Andrew Harp, Geoffrey Irving, Michael Isard, Yangqing Jia, Rafal Jozefowicz, Lukasz Kaiser, Manjunath Kudlur, Josh Levenberg, Dandelion Mané, Rajat Monga, Sherry Moore, Derek Murray, Chris Olah, Mike Schuster, Jonathon Shlens, Benoit Steiner, Ilya Sutskever, Kunal Talwar, Paul Tucker, Vincent Vanhoucke, Vijay Vasudevan, Fernanda Viégas, Oriol Vinyals, Pete Warden, Martin Wattenberg, Martin Wicke, Yuan Yu, and Xiaoqiang Zheng. TensorFlow: Large-scale machine learning on heterogeneous systems, 2015. Software available from tensorflow.org.

Rahul Agrawal, Archit Gupta, Yashoteja Prabhu, and Manik Varma. Multi-label learning with millions of labels: Recommending advertiser bid phrases for web pages. In *Proceedings of the 22nd International Conference on World Wide Web*, WWW '13, pp. 13–24, New York, NY, USA, 2013. Association for Computing Machinery.

Hesam Amoualian, Parantapa Goswami, Laurent Ach, Pradipto Das, and Pablo Montalvo. Sigir 2020 e-commerce workshop data challenge overview. In *Proceedings Proceedings of ACM SIGIR Workshop on eCommerce (SIGIR eCom'20). ACM*. ACM, 2020.

Evlampios Apostolidis, Eleni Adamantidou, Alexandros I. Metsai, Vasileios Mezaris, and Ioannis Patras. AC-SUM-GAN: Connecting actor-critic and generative adversarial networks for unsupervised video summarization,. *IEEE Transactions on Circuits and Systems for Video Technology*, 2020.

Rohit Babbar and Bernhard Schölkopf. Dismec: Distributed sparse machines for extreme multi-label classification. In *Proceedings of the Tenth ACM International Conference on Web Search and Data Mining*, WSDM '17, pp. 721–729, New York, NY, USA, 2017. Association for Computing Machinery.

Emanuel Ben Baruch, Tal Ridnik, Nadav Zamir, Asaf Noy, Itamar Friedman, Matan Protter, and Lihi Zelnik-Manor. Asymmetric loss for multi-label classification. *CoRR*, abs/2009.14119, 2020.

Bichitrananda Behera, G. Kumaravelan, and P. Kumar B. Performance evaluation of deep learning algorithms in biomedical document classification. In *2019 11th International Conference on Advanced Computing (ICoAC)*, pp. 220–224, 2019.

Fernando Benites and Elena Sapozhnikova. HARAM: A hierarchical ARAM neural network for large-scale text classification. In *2015 IEEE International Conference on Data Mining Workshop (ICDMW)*, pp. 847–854, 2015.

Kush Bhatia, Himanshu Jain, Purushottam Kar, Manik Varma, and Prateek Jain. Sparse local embeddings for extreme multi-label classification. In C. Cortes, N. Lawrence, D. Lee, M. Sugiyama, and R. Garnett (eds.), *Advances in Neural Information Processing Systems*, volume 28. Curran Associates, Inc., 2015.

Christopher M. Bishop. *Pattern Recognition and Machine Learning*. Information science and statistics. Springer, 5 edition, 2007.

M. J. Blosseville, Georges Hébrail, Marie-Gaëlle Monteil, and N. Pénot. Automatic document classification: Natural language processing, statistical analysis, and expert system techniques used together. In *Proceedings of the 15th Annual International ACM SIGIR Conference on Research and Development in Information Retrieval*, SIGIR '92, pp. 51–58, New York, NY, USA, 1992. Association for Computing Machinery.

Matthew R. Boutell, Jiebo Luo, Xipeng Shen, and Christopher M. Brown. Learning multi-label scene classification. *Pattern Recognition*, 37(9):1757–1771, 2004.

Klaus Brinker, Johannes Fürnkranz, and Eyke Hüllermeier. A unified model for multilabel classification and ranking. In *Proceedings of the 2006 Conference on ECAI 2006: 17th European Conference on Artificial Intelligence August 29 – September 1, 2006, Riva Del Garda, Italy*, pp. 489–493, NLD, 2006. IOS Press.

Trstenjak Bruno, Mikac Sasa, and Dzenana Donko. KNN with TF-IDF based framework for text categorization. *Procedia Engineering*, 69:1356–1364, 11 2013.

Wei-Cheng Chang, Hsiang-Fu Yu, Kai Zhong, Yiming Yang, and Inderjit S. Dhillon. The unknown benefits of using a soft-f1 loss in classification systems. *Towards Data Science*, Dec 2019. URL `https://towardsdatascience.com/the-unknown-benefits-of-using-a-soft-f1-loss-in-classification-systems-753902c0105d`.

Wei-Cheng Chang, Hsiang-Fu Yu, Kai Zhong, Yiming Yang, and Inderjit S. Dhillon. Taming pretrained transformers for extreme multi-label text classification. *Proceedings of the 26th ACM SIGKDD International Conference on Knowledge Discovery & Data Mining*, Jul 2020.

James J. Chen, Chen-An Tsai, Hojin Moon, Hongshik Ahn, John J. Young, and Chun-Houh Chen. Decision threshold adjustment in class prediction. *SAR and QSAR in Environmental Research*, 17(3):337–352, Jun 2006.

Wei-Ta Chu and Hung-Jui Guo. Movie genre classification based on poster images with deep neural networks. *Proceedings of the Workshop on Multimodal Understanding of Social, Affective and Subjective Attributes*, Oct 2017.

Amanda Clare and Ross D. King. Knowledge discovery in multi-label phenotype data. *Lecture Notes in Computer Science*, pp. 42–53, 2001.

Cornell-University. arXiv dataset and metadata of 1.7M+ scholarly papers across STEM. `kaggle.com/Cornell-University/arxiv`, 2021.

Washington Cunha, Vítor Mangaravite, Christian Gomes, Sérgio Canuto, Elaine Resende, Cecilia Nascimento, Felipe Viegas, Celso França, Wellington Santos Martins, Jussara M. Almeida, Thierson Rosa, Leonardo Rocha, and Marcos André Gonçalves. On the cost-effectiveness of neural and non-neural approaches and representations for text classification: A comprehensive comparative study. *Information Processing & Management*, 58(3):102481, 2021.

Krzysztof Dembczyński, Weiwei Cheng, and Eyke Hüllermeier. Bayes optimal multilabel classification via probabilistic classifier chains. In *Proceedings of the 27th International Conference on International Conference on Machine Learning*, ICML'10, pp. 279–286, Madison, WI, USA, 2010. Omnipress.

Jia Deng, Wei Dong, Richard Socher, Li-Jia Li, Kai Li, and Li Fei-Fei. ImageNet: A large-scale hierarchical image database. In *2009 IEEE Conference on Computer Vision and Pattern Recognition*, pp. 248–255, 2009.

Jacob Devlin, Ming-Wei Chang, Kenton Lee, and Kristina Toutanova. BERT: Pre-training of deep bidirectional transformers for language understanding. In *Proceedings of the 2019 Conference of the North American Chapter of the Association for Computational Linguistics: Human Language Technologies, Volume 1 (Long and Short Papers)*, pp. 4171–4186, Minneapolis, Minnesota, June 2019. Association for Computational Linguistics.

Ali Diba, Mohsen Fayyaz, Vivek Sharma, Manohar Paluri, Jurgen Gall, Rainer Stiefelhagen, and Luc Van Gool. Large Scale Holistic Video Understanding. *arXiv preprint arXiv:1904.11451v3*, 2019.

Jingcheng Du, Qingyu Chen, Yifan Peng, Yang Xiang, Cui Tao, and Zhiyong Lu. Ml-net: Multi-label classification of biomedical texts with deep neural networks. *Journal of the American Medical Informatics Association*, 26(11):1279–1285, Jun 2019.

Elad Eban, Mariano Schain, Alan Mackey, Ariel Gordon, Ryan Rifkin, and Gal Elidan. Scalable Learning of Non-Decomposable Objectives. In Aarti Singh and Jerry Zhu (eds.), *Proceedings of the 20th International Conference on Artificial Intelligence and Statistics*, volume 54 of *Proceedings of Machine Learning Research*, pp. 832–840. PMLR, 20–22 Apr 2017.

André Elisseeff and Jason Weston. A kernel method for multi-labelled classification. In *Proceedings of the 14th International Conference on Neural Information Processing Systems: Natural and Synthetic*, NIPS'01, pp. 681–687, Cambridge, MA, USA, 2001. MIT Press.

Mark Everingham, Luc Van Gool, Christopher KI Williams, John Winn, and Andrew Zisserman. The PASCAL visual object classes challenge 2007 (VOC2007) results. `http://www.pascal-network.org/challenges/VOC/voc2007/index.html`, 2007.

Ronald A. Fisher. On an absolute criterion for fitting frequency curves. *Messenger of Mathematics*, 41: 155–160, 1912.

Irving J. Good. Rational decisions. *Journal of the Royal Statistical Society: Series B (Methodological)*, 14 (1):107–114, Jan 1952.

Google. Feature vectors of images with MobileNet V2 (depth multiplier 1.00) trained on ImageNet (ILSVRC-2012-CLS). `https://tfhub.dev/google/imagenet/mobilenet_v2_100_224/feature_vector/4`, 2021.

Chuan Guo, Geoff Pleiss, Yu Sun, and Kilian Q. Weinberger. On calibration of modern neural networks. In Doina Precup and Yee Whye Teh (eds.), *Proceedings of the 34th International Conference on Machine Learning*, volume 70 of *Proceedings of Machine Learning Research*, pp. 1321–1330. PMLR, 06–11 Aug 2017.

Douglas Hanahan and Robert A. Weinberg. Hallmarks of cancer: The next generation. *Cell*, 144(5):646–674, Mar 2011.

Jun He, Liqun Wang, Liu Liu, Jiao Feng, and Hao Wu. Long document classification from local word glimpses via recurrent attention learning. *IEEE Access*, 7:40707–40718, 2019.

Jeremy Howard and Sebastian Ruder. Universal language model fine-tuning for text classification. *Proceedings of the 56th Annual Meeting of the Association for Computational Linguistics (Volume 1: Long Papers)*, 2018.

Hao Huang, Haihua Xu, Xianhui Wang, and Wushour Silamu. Maximum f1-score discriminative training criterion for automatic mispronunciation detection. *IEEE/ACM Transactions on Audio, Speech, and Language Processing*, 23(4):787–797, Apr 2015.

Huggingface. DistilBERT. `https://huggingface.co/transformers/model_doc/distilbert.html`, 2021.

David A Hull. *Information retrieval using statistical classification*. PhD thesis, Stanford University, 1994.

Eyke Hüllermeier, Johannes Fürnkranz, Weiwei Cheng, and Klaus Brinker. Label ranking by learning pairwise preferences. *Artificial Intelligence*, 172(16):1897–1916, 2008.

Himanshu Jain, Yashoteja Prabhu, and Manik Varma. Extreme multi-label loss functions for recommendation, tagging, ranking; other missing label applications. In *Proceedings of the 22nd ACM SIGKDD International Conference on Knowledge Discovery and Data Mining*, KDD '16, pp. 935–944, New York, NY, USA, 2016. Association for Computing Machinery.

Himanshu Jain, Venkatesh Balasubramanian, Bhanu Chunduri, and Manik Varma. Slice: Scalable linear extreme classifiers trained on 100 million labels for related searches. In *WSDM '19, February 11–15, 2019, Melbourne, VIC, Australia*. ACM, February 2019. Best Paper Award at WSDM '19.

Yacine Jernite, Anna Choromanska, and David Sontag. Simultaneous learning of trees and representations for extreme classification and density estimation. In *Proceedings of the 34th International Conference on Machine Learning - Volume 70*, ICML'17, pp. 1665–1674. JMLR.org, 2017.

Armand Joulin, Edouard Grave, Piotr Bojanowski, and Tomas Mikolov. Bag of tricks for efficient text classification. In *Proceedings of the 15th Conference of the European Chapter of the Association for Computational Linguistics: Volume 2, Short Papers*, pp. 427–431, Valencia, Spain, April 2017. Association for Computational Linguistics.

In-Ho Kang and GilChang Kim. Query type classification for web document retrieval. In *Proceedings of the 26th Annual International ACM SIGIR Conference on Research and Development in Informaion Retrieval*, SIGIR '03, pp. 64–71, New York, NY, USA, 2003. Association for Computing Machinery.

Oluwasanmi O. Koyejo, Nagarajan Natarajan, Pradeep K. Ravikumar, and Inderjit S. Dhillon. Consistent multilabel classification. In *Advances in Neural Information Processing Systems*, volume 28, pp. 3321–3329. Curran Associates, Inc., 2015.

Alex Krizhevsky, Ilya Sutskever, and Geoffrey E. Hinton. Imagenet classification with deep convolutional neural networks. *Communications of the ACM*, 60(6):84–90, May 2017.

Maksim Lapin, Matthias Hein, and Bernt Schiele. Top-k multiclass SVM. In *Proceedings of the 28th International Conference on Neural Information Processing Systems - Volume 1*, NIPS'15, pp. 325–333, Cambridge, MA, USA, 2015. MIT Press.

Maksim Lapin, Matthias Hein, and Bernt Schiele. Loss functions for top-k error: Analysis and insights. *2016 IEEE Conference on Computer Vision and Pattern Recognition (CVPR)*, Jun 2016.

Kristin Larsson, Ilona Silins, Yufan Guo, Anna Korhonen, Ulla Stenius, and Marika Berglund. Text mining for improved human exposure assessment. *Toxicology Letters*, 229:S119, Sep 2014.

Jens Lehmann, Robert Isele, Max Jakob, Anja Jentzsch, Dimitris Kontokostas, Pablo N Mendes, Sebastian Hellmann, Mohamed Morsey, Patrick Van Kleef, Sören Auer, and Christian Bizer. DBpedia – A large-scale, multilingual knowledge base extracted from Wikipedia. *Semantic Web*, 6(2):167–195, 2015.

Zhaoqi Leng, Mingxing Tan, Chenxi Liu, Ekin Dogus Cubuk, Jay Shi, Shuyang Cheng, and Dragomir Anguelov. PolyLoss: A polynomial expansion perspective of classification loss functions. In *International Conference on Learning Representations*, 2022.

Yuncheng Li, Yale Song, and Jiebo Luo. Improving pairwise ranking for multi-label image classification. *2017 IEEE Conference on Computer Vision and Pattern Recognition (CVPR)*, Jul 2017.

Tsung-Yi Lin, Michael Maire, Serge Belongie, James Hays, Pietro Perona, Deva Ramanan, Piotr Dollár, and C. Lawrence Zitnick. Microsoft coco: Common objects in context. *Lecture Notes in Computer Science*, pp. 740–755, 2014.

Tsung-Yi Lin, Priya Goyal, Ross Girshick, Kaiming He, and Piotr Dollar. Focal loss for dense object detection. *2017 IEEE International Conference on Computer Vision (ICCV)*, Oct 2017.

Zachary C. Lipton, Charles Elkan, and Balakrishnan Naryanaswamy. Optimal thresholding of classifiers to maximize f1 measure. *Lecture Notes in Computer Science*, pp. 225–239, 2014.

Jingzhou Liu, Wei-Cheng Chang, Yuexin Wu, and Yiming Yang. Deep learning for extreme multi-label text classification. *Proceedings of the 40th International ACM SIGIR Conference on Research and Development in Information Retrieval*, Aug 2017.

Shilong Liu, Lei Zhang, Xiao Yang, Hang Su, and Jun Zhu. Query2label: A simple transformer way to multi-label classification. *CoRR*, abs/2107.10834, 2021.

Eneldo Loza Mencia and Johannes Furnkranz. Pairwise learning of multilabel classifications with perceptrons. In *2008 IEEE International Joint Conference on Neural Networks (IEEE World Congress on Computational Intelligence)*, pp. 2899–2906, 2008.

Gjorgji Madjarov, Dragi Kocev, Dejan Gjorgjevikj, and Sašo Džeroski. An extensive experimental comparison of methods for multi-label learning. *Pattern recognition*, 45(9):3084–3104, 2012.

Christopher D. Manning, Prabhakar Raghavan, and Hinrich Schütze. *Introduction to Information Retrieval*. Cambridge University Press, 2008.

Aditya K Menon, Ankit Singh Rawat, Sashank Reddi, and Sanjiv Kumar. Multilabel reductions: what is my loss optimising? In H. Wallach, H. Larochelle, A. Beygelzimer, F. d'Alché-Buc, E. Fox, and R. Garnett (eds.), *Advances in Neural Information Processing Systems*, volume 32. Curran Associates, Inc., 2019.

Timo Milbich, Omair Ghori, Ferran Diego, and Björn Ommer. Unsupervised representation learning by discovering reliable image relations. *Pattern Recognition*, 102:107107, Jun 2020.

Felipe Kenji Nakano, Ricardo Cerri, and Celine Vens. Active learning for hierarchical multi-label classification. *Data Mining and Knowledge Discovery*, 34(5):1496–1530, 2020.

Neha. Movie genre from its poster. `https://www.kaggle.com/neha1703/movie-genre-from-its-poster`, 2018.

Rafael Padilla, Sergio L. Netto, and Eduardo A. B. da Silva. A survey on performance metrics for object-detection algorithms. In *2020 International Conference on Systems, Signals and Image Processing (IWSSIP)*, pp. 237–242, 2020.

Adam Paszke, Sam Gross, Francisco Massa, Adam Lerer, James Bradbury, Gregory Chanan, Trevor Killeen, Zeming Lin, Natalia Gimelshein, Luca Antiga, Alban Desmaison, Andreas Kopf, Edward Yang, Zachary DeVito, Martin Raison, Alykhan Tejani, Sasank Chilamkurthy, Benoit Steiner, Lu Fang, Junjie Bai, and Soumith Chintala. Pytorch: An imperative style, high-performance deep learning library. In H. Wallach, H. Larochelle, A. Beygelzimer, F. d'Alché-Buc, E. Fox, and R. Garnett (eds.), *Advances in Neural Information Processing Systems 32*, pp. 8024–8035. Curran Associates, Inc., 2019. URL `http://papers.neurips.cc/paper/9015-pytorch-an-imperative-style-high-performance-deep-learning-library.pdf`.

Yash Patel, Giorgos Tolias, and Jiri Matas. Recall@k surrogate loss with large batches and similarity mixup. *CVPR*, 2022.

Adler Perotte, Rimma Pivovarov, Karthik Natarajan, Nicole Weiskopf, Frank Wood, and Noémie Elhadad. Diagnosis code assignment: Models and evaluation metrics. *Journal of the American Medical Informatics Association*, 21(2):231–237, Mar 2014.

Yashoteja Prabhu, Anil Kag, Shrutendra Harsola, Rahul Agrawal, and Manik Varma. Parabel: Partitioned label trees for extreme classification with application to dynamic search advertising. In *Proceedings of the 2018 World Wide Web Conference*, WWW '18, pp. 993–1002, Republic and Canton of Geneva, CHE, 2018. International World Wide Web Conferences Steering Committee.

Harish G. Ramaswamy, Balaji Srinivasan Babu, Shivani Agarwal, and Robert C. Williamson. On the consistency of output code based learning algorithms for multiclass learning problems. In Maria Florina Balcan, Vitaly Feldman, and Csaba Szepesvári (eds.), *Proceedings of The 27th Conference on Learning Theory*, volume 35 of *Proceedings of Machine Learning Research*, pp. 885–902, Barcelona, Spain, 13–15 Jun 2014. PMLR.

Sashank J. Reddi, Satyen Kale, Felix Yu, Daniel Holtmann-Rice, Jiecao Chen, and Sanjiv Kumar. Stochastic negative mining for learning with large output spaces. In Kamalika Chaudhuri and Masashi Sugiyama (eds.), *Proceedings of the Twenty-Second International Conference on Artificial Intelligence and Statistics*, volume 89 of *Proceedings of Machine Learning Research*, pp. 1940–1949. PMLR, 16–18 Apr 2019.

Tal Ridnik, Hussam Lawen, Asaf Noy, Emanuel Ben Baruch, Gilad Sharir, and Itamar Friedman. Tresnet: High performance gpu-dedicated architecture. In *Proceedings of the IEEE/CVF Winter Conference on Applications of Computer Vision (WACV)*, pp. 1400–1409, January 2021.

Samuel Rota Bulò, Lorenzo Porzi, and Peter Kontschieder. In-place activated batchnorm for memory-optimized training of dnns. In *Proceedings of the IEEE Conference on Computer Vision and Pattern Recognition*, 2018.

Mark Sandler, Andrew Howard, Menglong Zhu, Andrey Zhmoginov, and Liang-Chieh Chen. MobileNetV2: Inverted residuals and linear bottlenecks. In *2018 IEEE/CVF Conference on Computer Vision and Pattern Recognition (CVPR)*, pp. 4510–4520, 06 2018.

Victor Sanh, Lysandre Debut, Julien Chaumond, and Thomas Wolf. DistilBERT, a distilled version of BERT: smaller, faster, cheaper and lighter. *CoRR*, abs/1910.01108, 2019.

Fumin Shen, Yadong Mu, Yang Yang, Wei Liu, Li Liu, Jingkuan Song, and Heng Tao Shen. Classification by retrieval: Binarizing data and classifiers. In *Proceedings of the 40th International ACM SIGIR Conference on Research and Development in Information Retrieval*, SIGIR '17, pp. 595–604, New York, NY, USA, 2017. Association for Computing Machinery.

Samuel L. Smith, Pieter-Jan Kindermans, and Quoc V. Le. Don't decay the learning rate, increase the batch size. *CoRR*, abs/1711.00489, 2017.

Hossein Soleimani and David J. Miller. Semisupervised, multilabel, multi-instance learning for structured data. *Neural Computation*, 29(4):1053–1102, 2017.

Ambuj Tewari and Peter L. Bartlett. On the consistency of multiclass classification methods. In Peter Auer and Ron Meir (eds.), *Learning Theory*, pp. 143–157, Berlin, Heidelberg, 2005. Springer Berlin Heidelberg.

Grigorios Tsoumakas and Ioannis Katakis. Multi-label classification: An overview. *International Journal of Data Warehousing and Mining (IJDWM)*, 3(3):1–13, 2007.

John Wilder Tukey. *Exploratory data analysis*. Addison-Wesley series in behavioral science : quantitative methods. Addison-Wesley, Reading, Mass. ;, 1977.

Willem Waegeman, Krzysztof Dembczyński, Arkadiusz Jachnik, Weiwei Cheng, and Eyke Hüllermeier. On the bayes-optimality of f-measure maximizers. *J. Mach. Learn. Res.*, 15(1):3333–3388, January 2014.

Jiang Wang, Yi Yang, Junhua Mao, Zhiheng Huang, Chang Huang, and Wei Xu. Cnn-rnn: A unified framework for multi-label image classification. In *Proceedings of the IEEE Conference on Computer Vision and Pattern Recognition (CVPR)*, June 2016.

Jingdong Wang, Ke Sun, Tianheng Cheng, Borui Jiang, Chaorui Deng, Yang Zhao, Dong Liu, Yadong Mu, Mingkui Tan, Xinggang Wang, and et al. Deep high-resolution representation learning for visual recognition. *IEEE Transactions on Pattern Analysis and Machine Intelligence*, pp. 1–1, 2020.

Xuanhui Wang, Cheng Li, Nadav Golbandi, Mike Bendersky, and Marc Najork. The lambdaloss framework for ranking metric optimization. In *Proceedings of The 27th ACM International Conference on Information and Knowledge Management (CIKM '18)*, pp. 1313–1322, 2018.

Yunchao Wei, Wei Xia, Min Lin, Junshi Huang, Bingbing Ni, Jian Dong, Yao Zhao, and Shuicheng Yan. Hcp: A flexible cnn framework for multi-label image classification. *IEEE Transactions on Pattern Analysis and Machine Intelligence*, 38(9):1901–1907, 2016.

Baoyuan Wu, Weidong Chen, Yanbo Fan, Yong Zhang, Jinlong Hou, Jie Liu, and Tong Zhang. Tencent ml-images: A large-scale multi-label image database for visual representation learning. *IEEE Access*, 7: 172683–172693, 2019.

Xi-Zhu Wu and Zhi-Hua Zhou. A unified view of multi-label performance measures. In Doina Precup and Yee Whye Teh (eds.), *Proceedings of the 34th International Conference on Machine Learning*, volume 70 of *Proceedings of Machine Learning Research*, pp. 3780–3788. PMLR, 06–11 Aug 2017.

Marek Wydmuch, Kalina Jasinska, Mikhail Kuznetsov, Róbert Busa-Fekete, and Krzysztof Dembczyński. A no-regret generalization of hierarchical softmax to extreme multi-label classification. In *Proceedings of the 32nd International Conference on Neural Information Processing Systems*, NIPS'18, pp. 6358–6368, Red Hook, NY, USA, 2018. Curran Associates Inc.

Jianxiong Xiao, James Hays, Krista A. Ehinger, Aude Oliva, and Antonio Torralba. Sun database: Large-scale scene recognition from abbey to zoo. In *2010 IEEE Computer Society Conference on Computer Vision and Pattern Recognition*, pp. 3485–3492, 2010.

Yiming Yang. An evaluation of statistical approaches to text categorization. *Information Retrieval*, 1:69–90, 2004.

Zhilin Yang, Zihang Dai, Yiming Yang, Jaime Carbonell, Russ R Salakhutdinov, and Quoc V Le. Xlnet: Generalized autoregressive pretraining for language understanding. In H. Wallach, H. Larochelle, A. Beygelzimer, F. d'Alché-Buc, E. Fox, and R. Garnett (eds.), *Advances in Neural Information Processing Systems*, volume 32, pp. 5753–5763. Curran Associates, Inc., 2019.

Ian E.H. Yen, Xiangru Huang, Wei Dai, Pradeep Ravikumar, Inderjit Dhillon, and Eric Xing. Ppdsparse: A parallel primal-dual sparse method for extreme classification. In *Proceedings of the 23rd ACM SIGKDD International Conference on Knowledge Discovery and Data Mining*, KDD '17, pp. 545–553, New York, NY, USA, 2017. Association for Computing Machinery.

Hsiang-Fu Yu, Prateek Jain, Purushottam Kar, and Inderjit S. Dhillon. Large-scale multi-label learning with missing labels. In *Proceedings of the 31st International Conference on International Conference on Machine Learning - Volume 32*, ICML'14, pp. I–593–I–601. JMLR.org, 2014.

Manzil Zaheer, Guru Guruganesh, Kumar Avinava Dubey, Joshua Ainslie, Chris Alberti, Santiago Ontanon, Philip Pham, Anirudh Ravula, Qifan Wang, Li Yang, and Amr Ahmed. Big bird: Transformers for longer sequences. In *Advances in Neural Information Processing Systems*, 2020.

Min-Ling Zhang and Zhi-Hua Zhou. Multilabel neural networks with applications to functional genomics and text categorization. *IEEE Transactions on Knowledge and Data Engineering*, 18(10):1338–1351, Oct 2006.

Min-Ling Zhang and Zhi-Hua Zhou. Ml-knn: A lazy learning approach to multi-label learning. *Pattern Recognition*, 40(7):2038–2048, Jul 2007.

Min-Ling Zhang and Zhi-Hua Zhou. A review on multi-label learning algorithms. *IEEE Transactions on Knowledge and Data Engineering*, 26(8):1819–1837, Aug 2014.

Tong Zhang. Statistical behavior and consistency of classification methods based on convex risk minimization. *The Annals of Statistics*, 32(1):56 – 85, 2004.

Xiang Zhang, Junbo Zhao, and Yann LeCun. Character-level convolutional networks for text classification. In *Proceedings of the 28th International Conference on Neural Information Processing Systems - Volume 1*, NIPS'15, pp. 649–657, Cambridge, MA, USA, 2015. MIT Press.

Zhi-Hua Zhou, Min-Ling Zhang, Sheng-Jun Huang, and Yu-Feng Li. Multi-instance multi-label learning. *Artificial Intelligence*, 176(1):2291 – 2320, 2012.

Feng Zhu, Hongsheng Li, Wanli Ouyang, Nenghai Yu, and Xiaogang Wang. Learning spatial regularization with image-level supervisions for multi-label image classification. In *Proceedings of the IEEE Conference on Computer Vision and Pattern Recognition (CVPR)*, July 2017.

Appendix A Evaluation Metrics

In our experimental evaluation, we consider a suite of metrics that are commonly used in the evaluation of multilabel classification to measure the effectiveness of multilabel prediction. These metrics are based on the confusion matrix and for which we provided smoothed surrogates to optimize directly (see Table 4).

When true positives and false positives are used, recall that $tp = \mathbb{1}_{\hat{\mathbf{y}} \geq t} \odot \mathbf{y}$ and $fp = \mathbb{1}_{\hat{\mathbf{y}} \geq t} \odot (\mathbb{1} - \mathbf{y})$, and thus a threshold t must be set. For Pascal-VOC, we set $t = 0.5$, as is commonly done in the early literature (Zhang & Zhou, 2014; Clare & King, 2001). In the recent literature, the chosen threshold at inference time can vary but was not found to be justified, we thus decide on neutral thresholds before training.

Extending F_1 to multiclass binary classification means deciding whether to pool classes. In a first pooled iteration, macro F_1 (Koyejo et al., 2015) equates to creating a single 2x2 confusion matrix for all classes:

$$F_1^{macro} = \frac{\sum^C 2tp_j}{2\sum^C tp_j + \sum^C fn_j + \sum^C fp_j}, \tag{9}$$

with $\sum^C(\cdot)$ as a short form of $\sum_{j=1}^C(\cdot)$, when summing over each class up to the C classes. Micro F_1 (Lipton et al., 2014; Koyejo et al., 2015) amounts to creating one confusion matrix per class or unpooling:

$$F_1^{micro} = \frac{1}{C}\sum_{j=1}^{C} \frac{2tp_j}{2tp_j + fn_j + fp_j} = \frac{1}{C}\sum_{j=1}^{C} F_1^j. \tag{10}$$

Weighted micro F_1 (Behera et al., 2019) is similar but includes weighing to account for class imbalance, i.e., weighing each class by the number of ground truth positives:

$$F_1^{weighted} = \frac{1}{C}\sum_{j=1}^{C} p_j F_1^j \quad \text{, where } p_j = \sum_i \mathbb{1}_{\mathbf{y_i^j}=1}. \tag{11}$$

We also define micro precision

$$P^{micro} = \frac{1}{C}\sum_{j=1}^{C} \frac{tp_j}{tp_j + fp_j}. \tag{12}$$

mean Average Precision (mAP) has different definitions. We use mAP as defined for the MS-COCO and Pascal-VOC datasets (Padilla et al., 2020). Traditionally, Precision and Recall is computed over the intersection of object detection boxes. We use a slightly modified mAP (e.g., in (Baruch et al., 2020)), where precision and recall are computed over the predictions of labels on the whole image. We first obtain the average precision over each class:

$$\begin{aligned} \mathrm{AP}_{\mathrm{all}} &= \sum_i \left(R_{i+1} - R_i\right) P_{\mathrm{interp}}\ (R_{i+1}) \\ P_{\mathrm{interp}}\ (R_{i+1}) &= \max_{\tilde{R}:\tilde{R} \geq R_{i+1}} P(\tilde{R}), \end{aligned} \tag{13}$$

and then compute mean Average Precision:

$$\mathrm{mAP}^{micro} = \frac{1}{C}\sum_{j=1}^{C} \mathrm{AP}_i. \tag{14}$$

We write micro here to be explicit, but it seems to be mostly computed at the micro level in the literature.

Appendix B Focal Loss definition

We write down the *focalLoss* (Lin et al., 2017), as it deals specifically with class imbalance and is used as a baseline due to its popularity in the multiclass domain.

$$\mathcal{L}_{FL} = -\alpha^{\mathrm{j}} \left(1 - \hat{y}^{\mathrm{j}}\right)^{\gamma} \log\left(\hat{y}^{\mathrm{j}}\right), \tag{15}$$

Table 4: Confusion matrix with our proposed smoothed confusion matrix entries, $\widetilde{tp}$, $\widetilde{fp}$, $\widetilde{fn}$ and $\widetilde{tn}$ and six derived loss functions that use these smoothed confusion matrix entries. $\mathcal{L}_{\widetilde{F1}}$ is used in our experiments.

	Condition positive	**Condition negative**	$\mathcal{L}_{\widetilde{Accuracy}} = \frac{\widetilde{tp}+\widetilde{tn}}{\widetilde{tp}+\widetilde{fp}+\widetilde{tn}+\widetilde{fn}}$
Predicted positive	True positive $\widetilde{tp} = \sum \mathbf{S}(\hat{\mathbf{y}}) \odot \mathbf{y}$	False positive $\widetilde{fp} = \sum \mathbf{S}(\hat{\mathbf{y}}) \odot (\mathbb{1} - \mathbf{y})$	$\mathcal{L}_{\widetilde{Precision}} = \frac{\widetilde{tp}}{\widetilde{tp}+\widetilde{fp}}$
Predicted negative	False negative $\widetilde{fn} = \sum(\mathbb{1} - \mathbf{S}(\hat{\mathbf{y}})) \odot \mathbf{y}$	True Negative $\widetilde{tn} = \sum(\mathbb{1} - \mathbf{S}(\hat{\mathbf{y}})) \odot (\mathbb{1} - \mathbf{y})$	$\mathcal{L}_{\widetilde{NPV}} = \frac{\widetilde{tn}}{\widetilde{tn}+\widetilde{fn}}$
	$\mathcal{L}_{\widetilde{Recall}} = \frac{\widetilde{tp}}{\widetilde{tp}+\widetilde{fn}}$	$\mathcal{L}_{\widetilde{Specificity}} = \frac{\widetilde{tn}}{\widetilde{fp}+\widetilde{tn}}$	$\mathcal{L}_{\widetilde{F1}} = \frac{2\widetilde{tp}}{2\widetilde{tp}+\widetilde{fn}+\widetilde{fp}}$

with α^j and γ hyperparameters. In the next section, we further specify the setup for focal loss and cross entropy as benchmarks for *unboundedF1* and *sigmoidF1*.

Appendix C Experimental Setup Details

moviePosters consists of images of movie posters and their genres (e.g., *action*, *comedy*) (Chu & Guo, 2017).[6] The posters and labels have been extracted from IMDB and the dataset was previously used for per-class, post-training thresholding (see Section 3). The genre labels in this dataset are not mutually exclusive and of varying counts per movie.

arXiv2020 is a subset of the newly created *arXiv dataset*[7] with over 1.7 million open source articles and their metadata. Our experiments use the abstracts and categories that are suitably non-mutually exclusive and of varying counts per example. The limited number of labeled classes render the older dataset unsuitable for our experiments. We write arXiv2020 for the subset of the *arXiv dataset* that only contains documents published in 2020. This results in around 26k documents. There is a longer history of using arXiv to create research datasets; the dataset we use is not to be confused with an earlier long document dataset that only features 11 classes (He et al., 2019), and was used in a recent long transformer publication (Zaheer et al., 2020).

pascal-VOC stands for Pascal Visual Object Classes Challenge (VOC 2007) (Everingham et al., 2007). It is an object recognition/segmentation dataset with 20 possible object classes and around 10K examples. Some multilabel classification literature for the image domain use object detection / segmentation datasets to perform multilabel classification:[8] MS-COCO, Pascal-VOC, NUS-WIDE, etc. (note that transformer models, which effectively distinguish the original objects on the image while predicting labels, perform better on this task (Liu et al., 2021)). Regarding Tresnet-m-21k (Ridnik et al., 2021), while an L and an XL version of the model exist, the code available online did not allow for correct loading of the weights.

We choose to ignore classes that are underrepresented, in order to give the model a fair chance at learning from at least a few examples. We define underrepresentation as a global irrelevance threshold b for classes: any class c that is represented less than b times is considered irrelevant. We decided to set an irrelevance threshold b on all datasets prior to conducting experiments, so as to not fine-tune for that feature. It was set to 1000 for both *arXiv2020* (145 of the original 155 classes remaining) and *moviePosters* (14 of the 28 classes remaining) and at 10 for *chemicalExposure* (all 38 classes remaining) and *cancerHallmarks* (all 33 classes remaining), in proportion to the number of classes and labels in each dataset. We used all classes for Pascal-VOC since we are comparing with benchmarks that also do so.

[6] Labels at `https://tinyurl.com/y7ydyedu` and images at `https://tinyurl.com/y7lfpvlx`.
[7] Available at `https://tinyurl.com/5kypspya`
[8] See `https://paperswithcode.com/task/multi-label-classification`

Regarding hyperparameters, for Pascal-VOC, we found $\{\beta = -0.75; \eta = 10.25\}$ to work best on mAP. For arXiv2020 and moviePosters, $\{\beta = 1; \eta = 9\}$ works best on weightedF1. These hyperparameters where tuned on the validation set and we report on the held out test set.

setup We performed our experiments on Amazon Web Services cloud machines with data parallelization on up to 4 GPUs *g4dn.12xlarge*, with TensorFlow 2 (Abadi et al., 2015) and PyTorch (Paszke et al., 2019) as a gradient-descent backend.

Appendix D Extended Results

The boxplots below show median and inter quartile range in the blue box.

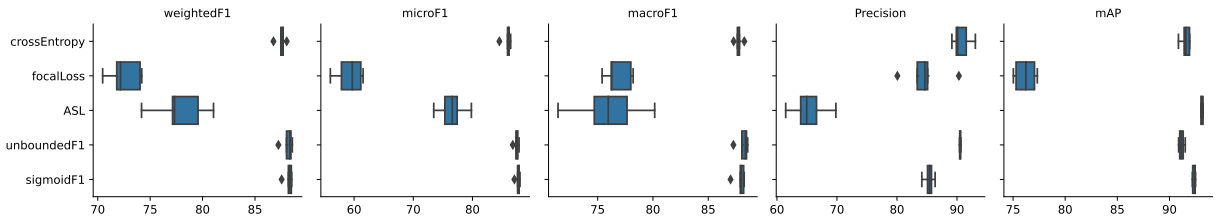

Figure 4: Tresnetm21K (CNN) on Pascal-VOC @0.5 (one outlier (<40) for unboundedF1 on each metric ignored for better visualization)

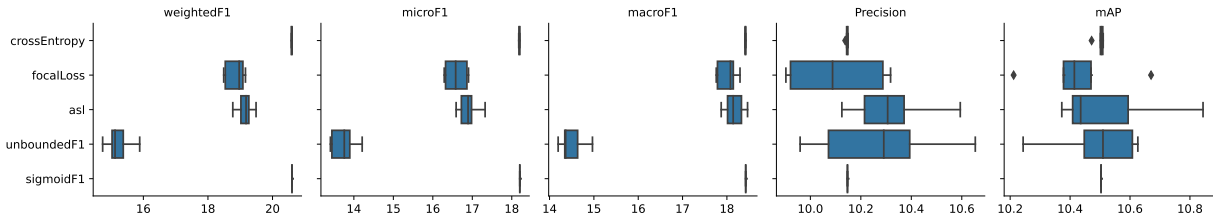

Figure 5: DistilBERT (NLP) on arXiv2020 @0.05.

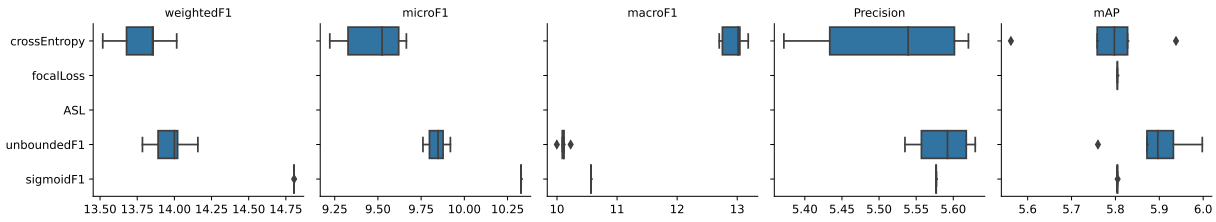

Figure 6: MobileNetV2 (CNN) on moviePosters @0.05 (zero values for focalLoss and ASL ignored for better visualization).

Appendix E Compute Time

Table 5: Average compute time over 100 epochs in minutes

	Pascal-VOC	arXiv2020	moviePosters
$\mathcal{L}_{\text{BCE}}$[1912]	112	341	58
$\mathcal{L}_{\text{FL}}$[2017]	108	428	59
$\mathcal{L}_{\text{ASL}}$[2020]	109	427	59
$\mathcal{L}_{\overline{F1}}$[ours]	116	381	58
$\mathcal{L}_{\widetilde{F1}}$[ours]	111	351	52

Appendix F Additional Experiments

Table 6: Descriptive statistics of all datasets.

	Type	Classes	Average label count	Number of examples
moviePosters	image	28	2.165	37,632
arXiv2020	text	155	1.888	26,558
chemExposure	text	38	6.116	3,661
cancerHallmarks	text	33	3.501	1,582
Pascal-VOC	image	20	1.560	9,963

ML-NET (Du et al., 2019) has an interesting multitask approach to *fit-algorithm-to-data* methods for multilabel learning with unknown label count on text. The cancerHallmark (Hanahan & Weinberg, 2011)[9] and chemicalExposure (Larsson et al., 2014)[10] datasets were used. The third dataset diagnosisCodes could not be obtained (neither from the authors of ML-NET nor of the original paper (Perotte et al., 2014)). We aggregate sentence labels to the whole description for cancerHallmarks and chemicalExposure, as was done for ML-NET.

Table 7: Multilabel classification performance@0.05 on a single run.

(a) DistilBERT (NLP) + classification head on cancerHallmarks.

Loss	weightedF1	microF1	macroF1	Precision
$\mathcal{L}_{\text{BCE}}$	0.0	0.0	0.0	0.0
$\mathcal{L}_{\text{FL}}$	10.8	19.0	4.4	7.1
$\mathcal{L}_{\overline{F1}}$	17.0	17.6	**9.8**	**8.9**
$\mathcal{L}_{\widetilde{F1}}$	**20.2**	**31.3**	9.5	5.9

(b) DistilBERT (NLP) + classification head on chemicalExposure.

Loss	weightedF1	microF1	macroF1	Precision
$\mathcal{L}_{\text{BCE}}$	5.1	5.8	1.2	4.7
$\mathcal{L}_{\text{FL}}$	26.8	34.8	9.3	13.0
$\mathcal{L}_{\overline{F1}}$	21.8	19.4	**13.3**	**15.5**
$\mathcal{L}_{\widetilde{F1}}$	**31.9**	**43.2**	11.3	9.1

For arXiv2020, moviePosters, cancerHallmarks and chemicalExposure, we saw after a few preparatory training rounds that almost only *sigmoidF1* had non-zero results for $t = 0.5$. Class representation is a lot more sparse for these dataset, we thus set the evaluation metrics threshold to a reasonable value of 0.05 and train

[9] Available at `https://github.com/sb895/Hallmarks-of-Cancer`

[10] Available at `https://github.com/sb895/chemical-exposure-information-corpus`

for 100 (arXiv2020, moviePosters) or 500 (cancerHallmarks and chemicalExposure) epochs until reaching convergence. Once thresholds were decided upon, no further threshold-hacking was performed. Note that a threshold of 0.8 on Pascal-VOC, as used by Baruch et al. (2020), does not alter the results.

On the smaller chemicalExposure and cancerHallmarks datasets, the *unboundedF1* loss delivers good results for macroF1 and Precision and the *sigmoidF1* loss leads to higher scores on the remainder of the metrics.

We observe that *unboundedF1* scores higher than *sigmoidF1* on macroF1 on the two small text datasets (chemicalExposure and cancerHallmarks). Since *unboundedF1* forgoes thresholding altogether, we hypothesize that *unboundedF1* develops tolerance for sparse datasets with low number of class instances.

Notably for the cancerHallmarks dataset, predictions from a model trained with cross-entropy do not reach high enough values to surpass the threshold and thus all metrics return zero values. This was further observed during experimentation, thus cross-entropy loss might not be a good fit for solving multilabel problems.